Gulf Journal of Mathematics
Vol 24, Issue 2 (2026) 1-15

ISSN: 2309-4966
https://doi.org/10.56947/vks8wp31

BÉZIER APPROXIMATION OF FUZZY PARABOLIC EQUATIONS

HARRAN ABDEL-FATTAH JABER ABUAMRO[1], FARAH AINI ABDULLAH[2,*], ALI FAREED JAMEEL[3], ADILA AIDA AZAHAR[4] and MUATH TALAL MAHMOUD ALZUBI[5]

Abstract. This study presents the Bézier Control Points Method for approximating fuzzy parabolic partial differential equations. The fuzzy problem is transformed into lower and upper parametric problems using a fuzzy level representation. Bernstein polynomial bases are employed to construct the approximate solutions, while the corresponding control points are determined through a collocation procedure. Two benchmark problems with known exact solutions are considered. The numerical results show close agreement between the approximate and exact solutions and small absolute errors. Comparisons with previously reported methods demonstrate the accuracy and computational effectiveness of the proposed approach.

Keywords. Fuzzy partial differential equations, fuzzy heat equation, Bézier Control Points Method, fuzzy z-cut
2020 Mathematics Subject Classification. Primary 65M70, 35K05; Secondary 03E72

1. Introduction

Fuzzy logic provides a robust mathematical framework for addressing uncertainty, ambiguity, and missing information in practical applications [38]. Fuzzy numbers are frequently employed to denote uncertain parameters, initial and boundary conditions, and other elements inherent in mathematical models [13]. The theory of fuzzy-valued functions and their differentiability has been advanced through several significant contributions. The concept of fuzzy differentiation was initially presented by Chang and Zadeh [12], succeeded by the development of fuzzy differential calculus by Dubois and Prade [14], which was grounded in Zadeh's extension principle, and the establishment of the fuzzy derivative by Seikkala [33]. Partial differential equations (PDEs) are crucial for modeling various physical and engineering phenomena, including heat transfer, diffusion, and wave propagation [9]. In real-world scenarios, the accessible data and model parameters are often not accurately defined and may encompass a certain level

Date: Received: Aug 13, 2026; Revised: Sep 9, 2026; Accepted: Sep 16, 2026.
* Corresponding author
© The Author(s) 2026. This article is licensed under a Creative Commons Attribution-NonCommercial-NoDerivatives 4.0 International License. To view a copy of the licence, visit https://creativecommons.org/licenses/by-nc-nd/4.0/.

of ambiguity. Fuzzy partial differential equations (FPDEs) offer an effective approach to address these issues by enabling the representation of parameters, initial conditions, or boundary conditions as fuzzy variables [10, 36]. Fuzzy parabolic partial differential equations (FPPDEs) are especially pertinent to heat conduction and diffusion-related issues that encompass uncertain parameters or fuzzy initial and boundary conditions [36]. Due to the inherent challenges in deriving exact solutions for FPDEs, the development of robust numerical and approximation methods has emerged as a significant area of research [33, 28, 22]. Various analytical and semi-analytical techniques have been employed to provide approximate solutions for fuzzy heat equations. [4] utilized the Adomian Decomposition Method (ADM), whereas [27] employed the Homotopy Perturbation Method (HPM). [24] utilized the Variational Iteration Method (VIM), whereas [26] presented the Optimal Homotopy Asymptotic Method (OHAM) for addressing this category of problems. [23] have recently utilized the Natural Adomian Decomposition Method (NADM). [32] additionally employed both ADM and VIM to address fuzzy heat-like equations featuring variable coefficients. Related VIM formulations for fuzzy fractional heat-like and wave-like equations are discussed in [21]. While these techniques yield acceptable approximate outcomes, their execution may require extensive symbolic computations, numerous iterative components, or the identification of appropriate auxiliary variables. Recent studies have further contributed to the development of fuzzy differential equations from a theoretical perspective [6] and to collocation-based numerical approximation techniques for differential and integral problems [34]. Consequently, there is a necessity for effective and adaptable approximation methods capable of representing fuzzy solutions inside a straightforward matrix-based computational framework. In this context, the Bézier Control Points Method (BCPM) has garnered interest as an efficient polynomial approximation technique due to its geometric properties, smooth approximation ability, and simple computing execution. This technique has been effectively utilized for ordinary differential equations, boundary value problems, delay differential equations, fuzzy delay differential equations, and crisp PDEs [15, 19, 39, 25]. Notwithstanding these uses, the majority of existing works on FPPDEs predominantly rely on decomposition, perturbation, or spline methodologies. To the authors' knowledge, the direct application of BCPM for formulating different lower and upper approximate solutions of FPPDEs inside the z-cut framework has not been sufficiently explored. This gap serves as the primary impetus for the current study.

This study develops an efficient computational formulation of the Bézier Control Points Method (BCPM) for solving linear fuzzy parabolic partial differential equations (FPPDEs) within the z-cut framework. The proposed approach is based on the standard BCPM and established principles of fuzzy set theory. The original fuzzy problem is transformed into corresponding lower and upper deterministic parametric problems, which are approximated using the Bernstein–Bézier representation. The unknown control points are then determined through a residual-based collocation procedure while incorporating the prescribed initial and boundary conditions.

The contribution of the present work does not lie in introducing new z-cut theory, Bernstein polynomials, or collocation techniques individually. Rather, it lies in integrating these established mathematical tools into a unified control-point formulation for constructing the lower and upper parametric solutions of fuzzy parabolic problems. To the best of our knowledge, the fuzzy form of the BCPM has not previously been employed to obtain approximate solutions for linear FPPDEs in this manner. The resulting formulation provides a systematic matrix-based computational framework for approximating fuzzy parabolic solutions and examining their lower–upper structure and numerical errors. The performance of the proposed method is assessed through fuzzy error analysis, benchmark problems with known exact solutions, and comparisons with previously reported numerical methods.

2. Analytical Framework of the Bézier Control Points Method

This section delineates the analytical-numerical framework of the proposed BCPM for addressing FPPDEs. The fuzzy problem is reformulated utilizing the z-cut representation, and the ensuing lower and upper parametric problems are approximated via Bernstein basis polynomials and collocation points.

2.1. Framework and Analysis of the Fuzzy Parabolic Problem.

Consider the general fuzzy parabolic partial differential equation given by:

$$\frac{\partial \widetilde{u}(x,t)}{\partial t} = \mathcal{N}(x,t,\widetilde{u},\widetilde{u}_x,\widetilde{u}_{xx}) \oplus \widetilde{f}(x,t), \qquad 0 < x < L, \quad 0 \le t \le T. \tag{2.1}$$

where $\widetilde{u}(x,t)$ denotes the unknown fuzzy-valued solution, $\widetilde{f}(x,t)$ is a fuzzy source term, and $\mathcal{N}$ represents a fuzzy differential operator [9, 10]. For each $z \in [0,1]$, the z-cut representation of the fuzzy solution is expressed as:

$$[\widetilde{u}(x,t)]^z = [\underline{u}(x,t;z), \overline{u}(x,t;z)]. \tag{2.2}$$

where $\underline{u}(x,t;z)$ and $\overline{u}(x,t;z)$ denote the lower and upper z-level bounds, respectively [13, 10]. Different notions of fuzzy differentiability are discussed in [7, 8]. Under the assumption that the endpoint functions possess the required classical derivatives, the z-level representations of the spatial derivatives for $r = 1, 2$ are given by:

$$\left[\frac{\partial^r \widetilde{u}}{\partial x^r}\right]^z = \left[\frac{\partial^r \underline{u}}{\partial x^r}, \frac{\partial^r \overline{u}}{\partial x^r}\right].$$

For uniformly parabolic operators, the diffusion coefficient $a(x,t;z)$ is assumed to satisfy the strictly positive condition $a(x,t;z) \ge a_0 > 0$ [29, 31]. Fuzzy heat equations under generalized Hukuhara differentiability are discussed in [3]. The associated fuzzy initial condition and general linear boundary conditions are defined as:

$$\widetilde{u}(x,0) = \widetilde{\psi}(x), \tag{2.3}$$

$$\lambda_k \odot \widetilde{u}(x_k,t) \oplus \eta_k \odot \widetilde{u}_x(x_k,t) = \widetilde{h}_k(t), \qquad k = 0, 1. \tag{2.4}$$

where $x_0 = 0$, $x_1 = L$, and the non-negative parameters satisfy $\lambda_k, \eta_k \ge 0$ with $\lambda_k + \eta_k > 0$. This general formulation encompasses Dirichlet, Neumann, and

Robin boundary conditions as special cases [29, 31]. The formulation of fuzzy Dirichlet conditions for heat transport problems has also been addressed in [18]. Applying the z-cut operation to the source term, initial condition, and boundary functions yields:

$$[\widetilde{f}(x,t)]^z = [\underline{f}(x,t;z), \overline{f}(x,t;z)], \qquad [\widetilde{\psi}(x)]^z = [\underline{\psi}(x;z), \overline{\psi}(x;z)],$$
$$[\widetilde{h}_k(t)]^z = [\underline{h}_k(t;z), \overline{h}_k(t;z)].$$

Given that the operator $\mathcal{N}$ may incorporate nonlinear or fuzzy-valued components, its z-level evaluation is constructed via standard interval arithmetic extensions [30]:

$$[\mathcal{N}(x,t,\widetilde{u},\widetilde{u}_x,\widetilde{u}_{xx})]^z = [\underline{\mathcal{N}}(x,t;z), \overline{\mathcal{N}}(x,t;z)]. \tag{2.5}$$

Consequently, for each fixed $z \in [0,1]$, the original fuzzy parabolic problem decouples into a pair of systemized, deterministic parametric partial differential equations:

$$\frac{\partial \underline{u}(x,t;z)}{\partial t} = \underline{\mathcal{N}}(x,t;z) + \underline{f}(x,t;z), \qquad \frac{\partial \overline{u}(x,t;z)}{\partial t} = \overline{\mathcal{N}}(x,t;z) + \overline{f}(x,t;z). \tag{2.6}$$

subject to the initial conditions:

$$\underline{u}(x,0;z) = \underline{\psi}(x;z), \qquad \overline{u}(x,0;z) = \overline{\psi}(x;z),$$

and boundary conditions:

$$\lambda_k \underline{u}(x_k,t;z) + \eta_k \frac{\partial \underline{u}(x_k,t;z)}{\partial x} = \underline{h}_k(t;z),$$
$$\lambda_k \overline{u}(x_k,t;z) + \eta_k \frac{\partial \overline{u}(x_k,t;z)}{\partial x} = \overline{h}_k(t;z), \qquad k = 0,1.$$

This decomposition establishes the lower and upper deterministic parametric models for every z-level, serving as the foundational analytical framework for the implementation of the Bézier Control Points Method [9, 10].

2.2. **Development of the Bézier Control Points Method.** Following the z-cut formulation in Section 2.1, the lower and upper parametric problems are approximated using the Bézier Control Points Method. The formulation is based on Bézier control-point approximations and their fuzzy representation [19, 20]. For $i = 0, 1, \ldots, n$ and $z \in [0,1]$, let the fuzzy Bernstein basis function be represented by

$$[\widetilde{B}_{i,n}(x)]^z = [\underline{B}_{i,n}(x;z), \overline{B}_{i,n}(x;z)], \qquad i = 0, \ldots, n,$$

with the corresponding Bernstein form

$$B_{i,n}(x) = \binom{n}{i} x^i (1-x)^{n-i}, \qquad 0 \le x \le 1. \tag{2.7}$$

At each z-level, the lower and upper Bernstein basis functions are assumed to retain the standard Bernstein polynomial form and its nonnegativity, partition-of-unity, and derivative properties. The Bernstein basis functions satisfy the

standard nonnegativity and partition-of-unity properties [17]:

$$\underline{B}_{i,n}(x;z) \geq 0, \qquad \overline{B}_{i,n}(x;z) \geq 0,$$
$$\sum_{i=0}^{n} \underline{B}_{i,n}(x;z) = \sum_{i=0}^{n} \overline{B}_{i,n}(x;z) = 1.$$

At each z-level, the fuzzy Bézier control points are represented by

$$[\widetilde{P}_i(t)]^z = [\underline{P}_i(t;z), \overline{P}_i(t;z)], \qquad i = 0, \ldots, n.$$

The fuzzy Bernstein–Bézier approximation is defined by

$$\widetilde{u}_n(x,t) = \bigoplus_{i=0}^{n} \left(\widetilde{P}_i(t) \odot \widetilde{B}_{i,n}(x) \right). \tag{2.8}$$

At each z-level, $[\widetilde{u}_n(x,t)]^z = [\underline{u}_n(x,t,z), \overline{u}_n(x,t,z)]$. Hence,

$$\underline{u}_n(x,t;z) = \sum_{i=0}^{n} \underline{P}_i(t;z)\underline{B}_{i,n}(x;z), \qquad \overline{u}_n(x,t;z) = \sum_{i=0}^{n} \overline{P}_i(t;z)\overline{B}_{i,n}(x;z). \tag{2.9}$$

The corresponding time derivatives are

$$\frac{\partial \underline{u}_n}{\partial t} = \sum_{i=0}^{n} \frac{\partial \underline{P}_i}{\partial t}\underline{B}_{i,n}(x;z), \qquad \frac{\partial \overline{u}_n}{\partial t} = \sum_{i=0}^{n} \frac{\partial \overline{P}_i}{\partial t}\overline{B}_{i,n}(x;z).$$

For $r = 1, 2$, the spatial derivatives are

$$\frac{\partial^r \underline{u}_n}{\partial x^r} = \sum_{i=0}^{n} \underline{P}_i(t;z)\frac{d^r \underline{B}_{i,n}(x;z)}{dx^r}, \qquad \frac{\partial^r \overline{u}_n}{\partial x^r} = \sum_{i=0}^{n} \overline{P}_i(t;z)\frac{d^r \overline{B}_{i,n}(x;z)}{dx^r}.$$

The first derivatives of the fuzzy Bernstein basis functions are [17]

$$\frac{d}{dx}\underline{B}_{i,n}(x;z) = n[\underline{B}_{i-1,n-1}(x;z) - \underline{B}_{i,n-1}(x;z)],$$
$$\frac{d}{dx}\overline{B}_{i,n}(x;z) = n[\overline{B}_{i-1,n-1}(x;z) - \overline{B}_{i,n-1}(x;z)].$$

Similarly,

$$\frac{d^2}{dx^2}\underline{B}_{i,n}(x;z) = n(n-1)[\underline{B}_{i-2,n-2}(x;z) - 2\underline{B}_{i-1,n-2}(x;z) + \underline{B}_{i,n-2}(x;z)],$$

and

$$\frac{d^2}{dx^2}\overline{B}_{i,n}(x;z) = n(n-1)[\overline{B}_{i-2,n-2}(x;z) - 2\overline{B}_{i-1,n-2}(x;z) + \overline{B}_{i,n-2}(x;z)].$$

Any basis function with an index outside its admissible range is taken to be zero [17]. Substituting the approximations into the lower and upper parametric equations gives the residual functions [37, 2]:

$$\underline{R}_n(x,t;z) = \frac{\partial \underline{u}_n}{\partial t} - \underline{\mathcal{N}}(x,t;z) - \underline{f}(x,t;z), \tag{2.10}$$

$$\overline{R}_n(x,t;z) = \frac{\partial \overline{u}_n}{\partial t} - \overline{\mathcal{N}}(x,t;z) - \overline{f}(x,t;z). \tag{2.11}$$

The control points are determined by imposing the residual equations at the interior Chebyshev–Lobatto points [35, 11]:

$$x_j = \frac{L}{2}\left(1 - \cos\frac{j\pi}{n}\right), \qquad j = 1, \ldots, n-1. \tag{2.12}$$

Thus,

$$\underline{R}_n(x_j, t; z) = 0, \qquad \overline{R}_n(x_j, t; z) = 0, \qquad j = 1, \ldots, n-1. \tag{2.13}$$

The boundary conditions are imposed at $x_0 = 0$ and $x_1 = L$:

$$\lambda_k \underline{u}_n(x_k, t; z) + \eta_k \frac{\partial \underline{u}_n(x_k, t; z)}{\partial x} = \underline{h}_k(t; z), \qquad k = 0, 1, \tag{2.14}$$

$$\lambda_k \overline{u}_n(x_k, t; z) + \eta_k \frac{\partial \overline{u}_n(x_k, t; z)}{\partial x} = \overline{h}_k(t; z), \qquad k = 0, 1. \tag{2.15}$$

Finally, the initial conditions are imposed at the full Chebyshev–Lobatto node set:

$$\underline{u}_n(x_j, 0; z) = \underline{\psi}(x_j; z), \qquad \overline{u}_n(x_j, 0; z) = \overline{\psi}(x_j; z), \qquad j = 0, \ldots, n. \tag{2.16}$$

The boundary equations are used to eliminate the dependent boundary control points, provided that the corresponding boundary system is nonsingular. The remaining control points are then determined from the interior collocation equations.

2.3. **Matrix Form and Determination of the Bernstein–Bézier Control Points.** For each $z \in [0, 1]$, the lower and upper fuzzy Bernstein–Bézier approximations are given by Eq. (2.9). The representation of differential-equation solutions in terms of Bézier control points follows the control-point formulations developed in [19, 39, 25, 37]. The initial control points are determined by imposing the z-cut initial conditions at the full collocation node set:

$$\sum_{i=0}^{n} \underline{P}_i(0; z)\underline{B}_{i,n}(x_j; z) = \underline{\psi}(x_j; z), \qquad \text{and}$$

$$\sum_{i=0}^{n} \overline{P}_i(0; z)\overline{B}_{i,n}(x_j; z) = \overline{\psi}(x_j; z), \qquad j = 0, \ldots, n.$$

This procedure determines the initial lower and upper control-point vectors through the corresponding Bernstein–Bézier representation [39, 25, 37]. For Dirichlet boundary conditions, the endpoint properties of the Bernstein basis [17] yield:

$$\underline{P}_0(t; z) = \underline{g}_0(t; z), \qquad \underline{P}_n(t; z) = \underline{g}_1(t; z),$$

$$\text{and} \qquad \overline{P}_0(t; z) = \overline{g}_0(t; z), \qquad \overline{P}_n(t; z) = \overline{g}_1(t; z).$$

Hence, the independent lower and upper control-point vectors are expressed as:

$$\underline{\mathbf{P}}_I(t; z) = [\underline{P}_1(t; z), \ldots, \underline{P}_{n-1}(t; z)]^T,$$

$$\text{and} \qquad \overline{\mathbf{P}}_I(t; z) = [\overline{P}_1(t; z), \ldots, \overline{P}_{n-1}(t; z)]^T.$$

After substituting the prescribed boundary control points into the interior collocation equations, the resulting equations are assembled into the reduced matrix system [39, 37]:

$$\mathcal{M}_I \frac{d\mathbf{Y}_I(t;z)}{dt} = \mathcal{A}_I \mathbf{Y}_I(t;z) + \mathbf{F}_I(t;z), \tag{2.17}$$

where

$$\mathbf{Y}_I(t;z) = \begin{bmatrix} \underline{\mathbf{P}}_I(t;z) \\ \overline{\mathbf{P}}_I(t;z) \end{bmatrix}, \qquad \mathbf{F}_I(t;z) = \begin{bmatrix} \underline{\mathbf{F}}_I(t;z) \\ \overline{\mathbf{F}}_I(t;z) \end{bmatrix}.$$

For the linear operator matrix A_I, define its positive and negative parts componentwise by:

$$A_I^+ = \max(A_I, 0), \qquad A_I^- = \min(A_I, 0).$$

Using standard interval arithmetic and interval extension [30], the corresponding block operator is represented by:

$$\mathcal{A}_I = \begin{bmatrix} A_I^+ & A_I^- \\ A_I^- & A_I^+ \end{bmatrix}. \tag{2.18}$$

This construction accounts for the interaction between the lower and upper endpoint systems under the interval representation [30]. If $\mathcal{M}_I$ is nonsingular, the reduced system becomes:

$$\frac{d\mathbf{Y}_I(t;z)}{dt} = \mathcal{B}_I \mathbf{Y}_I(t;z) + \mathbf{G}_I(t;z), \tag{2.19}$$

where $\mathcal{B}_I = \mathcal{M}_I^{-1}\mathcal{A}_I$ and $\mathbf{G}_I(t;z) = \mathcal{M}_I^{-1}\mathbf{F}_I(t;z)$. The corresponding initial condition is $\mathbf{Y}_I(0;z) = \mathbf{Y}_{I,0}(z)$. When $\mathcal{B}_I$ is independent of time, the reduced linear system admits the standard matrix-exponential representation [39, 37]:

$$\mathbf{Y}_I(t;z) = e^{\mathcal{B}_I t}\mathbf{Y}_{I,0}(z) + \int_0^t e^{\mathcal{B}_I(t-s)}\mathbf{G}_I(s;z)\,ds. \tag{2.20}$$

After restoring the prescribed boundary control points, the complete lower and upper fuzzy Bernstein–Bézier approximations are reconstructed using Eq. (2.9) [25, 37]. For nonlinear fuzzy parabolic problems, the same z-cut formulation is retained, while the nonlinear terms are evaluated through interval extension [30], leading to a nonlinear system for the lower and upper control points.

2.4. **Approximation Property of the Bernstein–Bézier Representation.** A convergence result for control-point approximations of fuzzy initial value problems was reported in [20]. However, the present study does not claim a general convergence theorem for the complete BCPM collocation scheme. Consistency, stability, and convergence of fuzzy differential-equation schemes require separate analysis [16]. For fixed t and z, let $u(\cdot,t;z) \in C([a,b])$ denote either the lower or upper parametric solution, and define $\xi = \frac{x-a}{b-a}$, $0 \le \xi \le 1$. The Bernstein approximation is given by:

$$B_n[u](x,t;z) = \sum_{i=0}^{n} u\left(a + \frac{i}{n}(b-a), t; z\right) \binom{n}{i} \xi^i (1-\xi)^{n-i}. \tag{2.21}$$

By the classical Bernstein approximation property [17]:

$$\lim_{n\to\infty} \|B_n[u](\cdot,t;z) - u(\cdot,t;z)\|_\infty = 0. \tag{2.22}$$

Thus, the Bernstein basis provides an appropriate approximation space for the proposed BCPM. This result concerns only the Bernstein–Bézier representation and does not constitute a convergence proof for the complete residual-based collocation scheme. Therefore, the numerical behavior of the method is assessed through the benchmark problems in the following section.

3. Numerical Examples

Two numerical examples are presented to evaluate the accuracy and computational performance of the proposed Bézier Control Points Method (BCPM) for solving fuzzy parabolic partial differential equations. Following the error representation used in [20], the absolute errors of the lower and upper approximate solutions are defined by

$$\underline{E}(x,t;z) = |\underline{U}(x,t;z) - \underline{u}_n(x,t;z)|, \qquad \overline{E}(x,t;z) = |\overline{U}(x,t;z) - \overline{u}_n(x,t;z)|. \tag{3.1}$$

where $\underline{U}(x,t;z)$ and $\overline{U}(x,t;z)$ denote the exact lower and upper solutions, respectively, while $\underline{u}_n(x,t;z)$ and $\overline{u}_n(x,t;z)$ denote the corresponding BCPM approximate solutions. These error measures are used throughout the numerical examples to assess the agreement between the approximate and exact solutions.

Example 3.1. This example considers the fuzzy heat equation reported in [5]:

$$\frac{\partial \widetilde{u}}{\partial t}(x,t) - \frac{1}{2}x^2\frac{\partial^2 \widetilde{u}}{\partial x^2}(x,t) = 0, \qquad 0 < x < 1, \quad 0 < t < 1. \tag{3.2}$$

The fuzzy initial condition is given by:

$$\widetilde{u}(x,0) = \widetilde{\lambda}x^2, \qquad 0 \le x \le 1, \tag{3.3}$$

where the fuzzy parameter $\widetilde{\lambda}$ is represented by the z-cut:

$$[\widetilde{\lambda}]^z = [\underline{\lambda}(z), \overline{\lambda}(z)] = [z-1, 1-z], \qquad z \in [0,1].$$

Hence, the lower and upper initial conditions are expressed as:

$$\underline{u}(x,0;z) = (z-1)x^2, \qquad \overline{u}(x,0;z) = (1-z)x^2.$$

Accordingly, the fuzzy problem is reduced to the lower and upper z-level deterministic equations:

$$\frac{\partial \underline{u}}{\partial t}(x,t;z) - \frac{1}{2}x^2\frac{\partial^2 \underline{u}}{\partial x^2}(x,t;z) = 0, \qquad 0 < x < 1, \quad 0 < t < 1, \tag{3.4}$$

$$\frac{\partial \overline{u}}{\partial t}(x,t;z) - \frac{1}{2}x^2\frac{\partial^2 \overline{u}}{\partial x^2}(x,t;z) = 0, \qquad 0 < x < 1, \quad 0 < t < 1. \tag{3.5}$$

The corresponding exact lower and upper solutions are:

$$\underline{U}(x,t;z) = (z-1)x^2e^t, \qquad \overline{U}(x,t;z) = (1-z)x^2e^t. \tag{3.6}$$

Applying the BCPM formulation developed in Sections 2.1–2.3 with degree $n = 10$, the lower and upper approximate solutions take the form:

$$\underline{u}_{10}(x,t;z) = \sum_{i=0}^{10} \underline{P}_i(t;z)\underline{B}_{i,10}(x;z), \qquad \overline{u}_{10}(x,t;z) = \sum_{i=0}^{10} \overline{P}_i(t;z)\overline{B}_{i,10}(x;z). \tag{3.7}$$

Using the residual collocation formulation in Eqs. (2.10)–(2.13) together with the initial conditions in Eq. (2.16), the degree-10 lower and upper control points are obtained. At $t = 0.6$, the lower control points are:

$$\begin{aligned}
&\underline{P}_0(0.6;z) = 0, \quad \underline{P}_1(0.6;z) = 0, \quad \underline{P}_2(0.6;z) = 0.040491528898(z-1),\\
&\underline{P}_3(0.6;z) = 0.121474586693(z-1), \quad \underline{P}_4(0.6;z) = 0.242949173385(z-1),\\
&\underline{P}_5(0.6;z) = 0.404915288976(z-1), \quad \underline{P}_6(0.6;z) = 0.607372933464(z-1),\\
&\underline{P}_7(0.6;z) = 0.850322106849(z-1), \quad \underline{P}_8(0.6;z) = 1.133762809132(z-1),\\
&\underline{P}_9(0.6;z) = 1.457695040312(z-1), \quad \underline{P}_{10}(0.6;z) = 1.822118800391(z-1).
\end{aligned}$$

The corresponding upper control points at $t = 0.6$ are:

$$\begin{aligned}
&\overline{P}_0(0.6;z) = 0, \quad \overline{P}_1(0.6;z) = 0, \quad \overline{P}_2(0.6;z) = 0.040491528898(1-z),\\
&\overline{P}_3(0.6;z) = 0.121474586693(1-z), \quad \overline{P}_4(0.6;z) = 0.242949173385(1-z),\\
&\overline{P}_5(0.6;z) = 0.404915288976(1-z), \quad \overline{P}_6(0.6;z) = 0.607372933464(1-z),\\
&\overline{P}_7(0.6;z) = 0.850322106849(1-z), \quad \overline{P}_8(0.6;z) = 1.133762809132(1-z),\\
&\overline{P}_9(0.6;z) = 1.457695040312(1-z), \quad \overline{P}_{10}(0.6;z) = 1.822118800391(1-z).
\end{aligned}$$

The proposed BCPM is evaluated at $x = 0.4$ and $t = 0.6$ for the levels $z = 0, 0.2, 0.4, 0.6, 0.8$, and 0.9. The approximate lower and upper solutions are compared with the corresponding exact solutions using the absolute errors defined in Eq. (3.1). For comparison, the results reported in [5], obtained using the tenth-order OHAM with a single convergent control parameter, are also considered. The results are presented in Tables 1–2 and Figures 1–4.

TABLE 1. Exact and approximate lower solutions and their absolute errors obtained by the BCPM with $n = 10$ at $x = 0.4$, $t = 0.6$, for selected z-levels in $[0, 1]$.

z	Exact lower solution	BCPM lower approximation	BCPM lower absolute error	OHAM lower absolute error
0	−0.291539008062	−0.291539008062	$3.3306691 \times 10^{-15}$	$1.1157741 \times 10^{-14}$
0.2	−0.233231206450	−0.233231206450	$2.6645353 \times 10^{-15}$	$1.7693896 \times 10^{-10}$
0.4	−0.174923404837	−0.174923404837	$1.9706459 \times 10^{-15}$	1.7751545×10^{-6}
0.6	−0.116615603225	−0.116615603225	$1.3322676 \times 10^{-15}$	$8.8469482 \times 10^{-11}$
0.8	−0.058307801612	−0.058307801612	$6.5919492 \times 10^{-16}$	1.6842284×10^{-9}
0.9	−0.029153900806	−0.029153900806	$3.2959746 \times 10^{-16}$	2.4648947×10^{-9}

Tables 1 and 2 show very close agreement between the exact and BCPM lower and upper solutions at $x = 0.4$ and $t = 0.6$. The absolute errors obtained by the BCPM range from approximately 3.30×10^{-16} to 3.33×10^{-15}, indicating high numerical accuracy at the selected test point. Furthermore, the BCPM errors are smaller than the corresponding OHAM errors for all the considered z-levels. The lower and upper solutions have equal magnitudes and opposite signs because

TABLE 2. Exact and approximate upper solutions and their absolute errors obtained by the BCPM with $n = 10$ at $x = 0.4$, $t = 0.6$, for selected z-levels in $\in [0, 1]$.

z	Exact upper solution	BCPM upper approximation	BCPM upper absolute error	OHAM upper absolute error
0	0.291539008062	0.291539008062	$3.3306691 \times 10^{-15}$	$1.1157741 \times 10^{-14}$
0.2	0.233231206450	0.233231206450	$2.6645353 \times 10^{-15}$	$1.7693896 \times 10^{-10}$
0.4	0.174923404837	0.174923404837	$1.9706459 \times 10^{-15}$	1.7751545×10^{-6}
0.6	0.116615603225	0.116615603225	$1.3322676 \times 10^{-15}$	$8.8469482 \times 10^{-11}$
0.8	0.058307801612	0.058307801612	$6.5919492 \times 10^{-16}$	1.6842284×10^{-9}
0.9	0.029153900806	0.029153900806	$3.2959746 \times 10^{-16}$	2.4648947×10^{-9}

the fuzzy parameter is represented by the symmetric interval $[z - 1, 1 - z]$. As z approaches one, both solution branches converge to zero.

In this example, the uncertain parameter is represented by a triangular fuzzy number with parameters $(-1, 0, 1)$ [40]. Accordingly, its exact membership function is triangular; the displayed plots show the sampled levels.

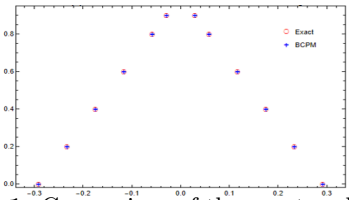


Figure 1. Comparison of the exact and BCPM approximate lower and upper solutions at $x = 0.4$, $t = 0.6$, and degree $n = 10$ for $z \in [0, 1]$.

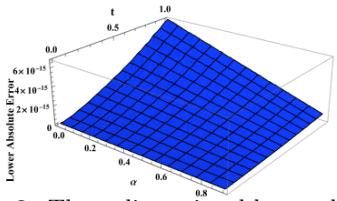


Figure 2. Three-dimensional lower absolute errors of the BCPM solutions at $x = 0.4$ and degree $n = 10$ for $z, t \in [0, 1]$.

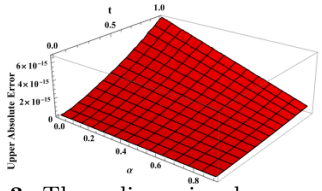


Figure 3. Three-dimensional upper absolute errors of the BCPM solutions at $x = 0.4$ and degree $n = 10$ for $z, t \in [0, 1]$.

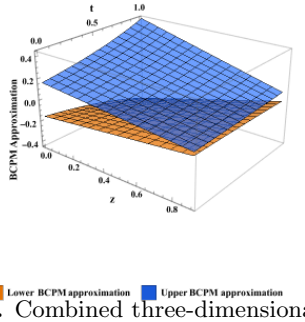


Figure 4. Combined three-dimensional plot of the lower and upper exact and BCPM approximate solutions at $x = 0.4$ and degree $n = 10$ for $z, t \in [0, 1]$.

Figure 1 shows close agreement between the exact and BCPM lower and upper solutions over the considered z-levels, consistent with Tables 1 and 2. Figures 2 and 3 show that the corresponding lower and upper absolute errors remain very small over the plotted domain. Figure 4 illustrates the combined lower and upper BCPM approximations, which preserve the required fuzzy ordering. Overall, Figures 1–4 support the numerical accuracy of the proposed method.

Example 3.2. This example considers the fuzzy parabolic problem presented in Example 4.1 of [1]:

$$\frac{\partial \widetilde{w}}{\partial t}(x, t) - \frac{\partial^2 \widetilde{w}}{\partial x^2}(x, t) = 0, \qquad 0 < x < 1, \quad t > 0, \tag{3.8}$$

subject to the homogeneous boundary conditions:

$$\widetilde{w}(0, t) = \widetilde{w}(1, t) = 0, \qquad t > 0, \tag{3.9}$$

and the fuzzy initial condition:

$$\widetilde{w}(x,0) = \widetilde{\lambda}\cos\left(\pi x - \frac{\pi}{2}\right), \qquad 0 < x < 1, \tag{3.10}$$

where the fuzzy parameter $\widetilde{\lambda}$ is represented by the z-cut:

$$[\widetilde{\lambda}]^z = [\underline{\lambda}(z), \overline{\lambda}(z)] = [z-1, 1-z], \qquad z \in [0,1].$$

Hence, the lower and upper initial conditions are given by:

$$\underline{w}(x,0;z) = (z-1)\cos\left(\pi x - \frac{\pi}{2}\right), \qquad \overline{w}(x,0;z) = (1-z)\cos\left(\pi x - \frac{\pi}{2}\right).$$

The corresponding exact lower and upper solutions are expressed as:

$$\underline{W}(x,t;z) = (z-1)e^{-\pi^2 t}\cos\left(\pi x - \frac{\pi}{2}\right), \tag{3.11}$$

$$\overline{W}(x,t;z) = (1-z)e^{-\pi^2 t}\cos\left(\pi x - \frac{\pi}{2}\right). \tag{3.12}$$

Applying the BCPM formulation developed in Sections 2.1–2.3 with degree $n = 5$, the lower and upper approximate solutions take the form:

$$\underline{w}_5(x,t;z) = \sum_{i=0}^{5} \underline{P}_i(t;z)\underline{B}_{i,5}(x;z), \qquad \overline{w}_5(x,t;z) = \sum_{i=0}^{5} \overline{P}_i(t;z)\overline{B}_{i,5}(x;z). \tag{3.13}$$

Using the residual collocation equations in Eqs. (2.10)–(2.13), together with the boundary and initial conditions, the degree-5 control points are obtained.

$$\underline{P}_0 = \underline{P}_5 = 0, \qquad \overline{P}_0 = \overline{P}_5 = 0.$$

At $t = 0.02$, the lower interior control points are obtained as:

$$\underline{P}_1 = 0.513432894947(z-1), \qquad \underline{P}_2 = \underline{P}_3 = 1.054701128234(z-1),$$
$$\underline{P}_4 = 0.513432894947(z-1).$$

The corresponding upper interior control points are:

$$\overline{P}_1 = 0.513432894947(1-z), \qquad \overline{P}_2 = \overline{P}_3 = 1.054701128234(1-z),$$
$$\overline{P}_4 = 0.513432894947(1-z).$$

The numerical results are evaluated at $x = \frac{1}{3}$ and $t = 0.02$ for the selected z-levels. The approximate solutions are compared with the exact solutions using the absolute errors defined in Eq. (3.1). For comparison, the results reported in [1] are also considered. In [1], a cubic non-polynomial spline method with tensor-product formulation was applied using $h = \frac{1}{3}$ and $k = 0.01$, leading to an algebraic system of size 16×16. The comparison is performed at the same x, t, and z-levels. The results are presented in Tables 3–4 and Figures 5–8.

Tables 3 and 4 show close agreement between the exact and BCPM lower and upper solutions at $x = \frac{1}{3}$ and $t = 0.02$. The largest BCPM absolute error is 1.0723233×10^{-4} at $z = 0$, and the error gradually decreases to zero as z approaches one. This behavior is due to the factors $z - 1$ and $1 - z$, which decrease in magnitude as the fuzzy level increases. The BCPM errors are smaller than the corresponding NPSM errors at all the considered z-levels. In particular, at $z = 0$, the NPSM error is approximately 93 times the BCPM error. Therefore,

TABLE 3. Exact and approximate lower solutions and their absolute errors obtained by the BCPM with $n = 5$ at $x = \frac{1}{3}$, $t = 0.02$, for $z \in [0, 1]$.

z	Exact lower solution	BCPM lower approximation	BCPM lower absolute error	NPSM lower absolute error
0.0	−0.710893162454	−0.711000394788	1.0723233×10^{-4}	1.000×10^{-2}
0.1	−0.639803846208	−0.639900355309	9.65091×10^{-5}	9.096×10^{-3}
0.2	−0.568714529963	−0.568800315830	8.5785867×10^{-5}	8.085×10^{-3}
0.3	−0.497625213718	−0.497700276351	7.5062634×10^{-5}	7.075×10^{-3}
0.4	−0.426535897472	−0.426600236873	6.43394×10^{-5}	6.064×10^{-3}
0.5	−0.355446581227	−0.355500197394	5.3616167×10^{-5}	5.053×10^{-3}
0.6	−0.284357264982	−0.284400157915	4.2892934×10^{-5}	4.043×10^{-3}
0.7	−0.213267948736	−0.213300118436	3.21697×10^{-5}	3.032×10^{-3}
0.8	−0.142178632491	−0.142200078958	2.1446467×10^{-5}	2.021×10^{-3}
0.9	−0.071089316245	−0.071100039479	1.0723233×10^{-5}	1.011×10^{-3}
1.0	0	0	0	0

TABLE 4. Exact and approximate upper solutions and their absolute errors obtained by the BCPM with $n = 5$ at $x = \frac{1}{3}$, $t = 0.02$, for $z \in [0, 1]$.

z	Exact upper solution	BCPM upper approximation	BCPM upper absolute error	NPSM upper absolute error
0.0	0.710893162454	0.711000394788	1.0723233×10^{-4}	1.000×10^{-2}
0.1	0.639803846208	0.639900355309	9.65091×10^{-5}	9.096×10^{-3}
0.2	0.568714529963	0.568800315830	8.5785867×10^{-5}	8.085×10^{-3}
0.3	0.497625213718	0.497700276351	7.5062634×10^{-5}	7.075×10^{-3}
0.4	0.426535897472	0.426600236873	6.43394×10^{-5}	6.064×10^{-3}
0.5	0.355446581227	0.355500197394	5.3616167×10^{-5}	5.053×10^{-3}
0.6	0.284357264982	0.284400157915	4.2892934×10^{-5}	4.043×10^{-3}
0.7	0.213267948736	0.213300118436	3.21697×10^{-5}	3.032×10^{-3}
0.8	0.142178632491	0.142200078958	2.1446467×10^{-5}	2.021×10^{-3}
0.9	0.071089316245	0.071100039479	1.0723233×10^{-5}	1.011×10^{-3}
1.0	0	0	0	0

the fifth-degree BCPM provides higher accuracy at the selected comparison point using six Bézier control points.

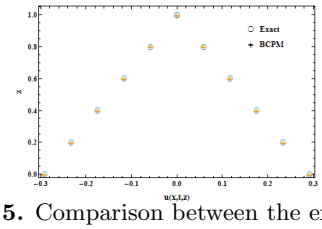


Figure 5. Comparison between the exact and approximate lower and upper solutions obtained by the BCPM with $n = 5$ at $x = \frac{1}{3}$, $t = 0.02$, for $z \in [0, 1]$.

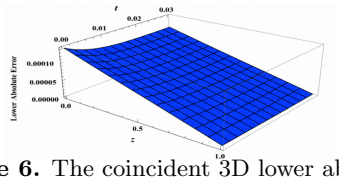


Figure 6. The coincident 3D lower absolute errors obtained by the BCPM with $N = 5$ at $x = \frac{1}{3}$, for $0 \le z \le 1$ and $0 \le t \le 0.03$.

Figure 5 shows close agreement between the exact and BCPM lower and upper solutions over the considered z-levels. Figures 6 and 7 show that the corresponding lower and upper absolute errors remain small over the plotted domain. Figure 8 illustrates the combined lower and upper BCPM approximations, which preserve the required fuzzy ordering. Overall, Figures 5–8 support the numerical accuracy of the proposed method.

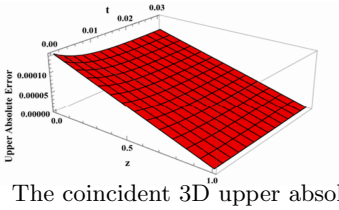


Figure 7. The coincident 3D upper absolute errors obtained by the BCPM with $N = 5$ at $x = \frac{1}{3}$, for $0 \le z \le 1$ and $0 \le t \le 0.03$.

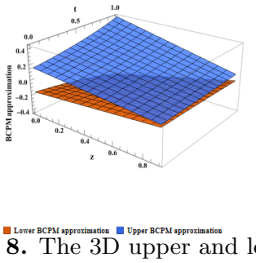


Figure 8. The 3D upper and lower approximate solutions obtained by the BCPM with $N = 5$ at $x = \frac{1}{3}$, for $0 \le z \le 1$ and $0 \le t \le 0.03$.

4. Conclusion

In this study, the Bézier Control Points Method (BCPM) was applied to approximate fuzzy parabolic partial differential equations. Using the z-cut representation, the fuzzy problem was reduced to lower and upper parametric problems. The numerical results showed close agreement between the BCPM approximations and the exact solutions, with small lower and upper absolute errors. For the considered examples and test points, the BCPM produced smaller errors than the compared methods reported in the literature. The approximate solutions also preserved the required fuzzy lower–upper ordering. These results demonstrate the effectiveness of the BCPM for the fuzzy parabolic problems examined in this study. The Bernstein–Bézier representation provides an appropriate approximation framework, while a rigorous convergence analysis of the complete BCPM collocation scheme remains a subject for future theoretical investigation.

References

1. Abud, A. H., Noman, L. M., & Bakheet, A. (2026). A developed non-polynomial spline method for solving fuzzy partial differential equations. *Int. J. Neutrosophic Sci.*, 27(1), 272–277. https://doi.org/10.54216/IJNS.270124
2. Akyüz-Daşcıoğlu, A., & Işler, N. (2013). Bernstein collocation method for solving nonlinear differential equations. *Math. Comput. Appl.*, 18(3), 293–300. https://doi.org/10.3390/mca18030293
3. Allahviranloo, T., Gouyandeh, Z., Armand, A., & Hasanoglu, A. (2015). On fuzzy solutions for heat equation based on generalized Hukuhara differentiability. *Fuzzy Sets and Systems*, 265, 1–23. https://doi.org/10.1016/j.fss.2014.11.009
4. Allahviranloo, T., & Taheri, N. (2009). An analytic approximation to the solution of fuzzy heat equation by Adomian decomposition method. *Int. J. Contemp. Math. Sci.*, 4(3), 105–114. https://www.m-hikari.com/ijcms-password2009/1-4-2009/allahviranlooIJCMS1-4-2009.pdf
5. Altaie, S., Jameel, A. F., & Saaban, A. (2019). A single convergent control parameter optimal homotopy asymptotic method approximate-analytical solution of fuzzy heat equation. *ASM Sci. J.*, 12(Special Issue 5), 42–47. https://www.akademisains.gov.my/asmsj/?mdocs-file=4175
6. Bechayeb, R., Maazouz, K., Bellabes, Z., & Rodríguez-López, R. (2026). New results of global existence and uniqueness for fuzzy fractional integro-differential equations. *Gulf J. Math.*, 23(1), 1–14. https://doi.org/10.56947/xzc41s28
7. Bede, B., & Gal, S. G. (2005). Generalizations of the differentiability of fuzzy-number-valued functions with applications to fuzzy differential equations. *Fuzzy Sets and Systems*, 151(3), 581–599. https://doi.org/10.1016/j.fss.2004.08.001

8. Bede, B., & Stefanini, L. (2013). Generalized differentiability of fuzzy-valued functions. *Fuzzy Sets and Systems*, 230, 119–141. https://doi.org/10.1016/j.fss.2012.10.003
9. Bertone, A. M., Jafelice, R. M., de Barros, L. C., & Bassanezi, R. C. (2013). On fuzzy solutions for partial differential equations. *Fuzzy Sets and Systems*, 219, 68–80. https://doi.org/10.1016/j.fss.2012.12.002
10. Buckley, J. J., & Feuring, T. (1999). Introduction to fuzzy partial differential equations. *Fuzzy Sets and Systems*, 105(2), 241–248. https://doi.org/10.1016/S0165-0114(98)00323-6
11. Canuto, C., Hussaini, M. Y., Quarteroni, A., & Zang, T. A. (2006). *Spectral methods: Fundamentals in single domains*. Springer. https://doi.org/10.1007/978-3-540-30726-6
12. Chang, S. S. L., & Zadeh, L. A. (1972). On fuzzy mapping and control. *IEEE Trans. Systems Man Cybernet.*, SMC-2(1), 30–34. https://doi.org/10.1109/TSMC.1972.5408553
13. Dijkman, J. G., van Haeringen, H., & de Lange, S. J. (1983). Fuzzy numbers. *J. Math. Anal. Appl.*, 92(2), 301–341. https://doi.org/10.1016/0022-247X(83)90253-6
14. Dubois, D., & Prade, H. (1982). Towards fuzzy differential calculus part 3: Differentiation. *Fuzzy Sets and Systems*, 8(3), 225–233. https://doi.org/10.1016/S0165-0114(82)80001-8
15. Evrenosoglu, M., & Somali, S. (2008). Least squares methods for solving singularly perturbed two-point boundary value problems using Bézier control points. *Appl. Math. Lett.*, 21(10), 1029–1032. https://doi.org/10.1016/j.aml.2007.10.021
16. Ezzati, R., Maleknejad, K., Khezerloo, S., & Khezerloo, M. (2015). Convergence, consistency and stability in fuzzy differential equations. *Iran. J. Fuzzy Syst.*, 12(3), 95–112. https://ijfs.usb.ac.ir/article_2021_27827fb7f621d2c20415fb8f401902e5.pdf
17. Farouki, R. T. (2012). The Bernstein polynomial basis: A centennial retrospective. *Comput. Aided Geom. Design*, 29(6), 379–419. https://doi.org/10.1016/j.cagd.2012.03.001
18. Gasilov, N. A., Amrahov, Ş. E., & Fatullayev, A. G. (2016). On a solution of the fuzzy Dirichlet problem for the heat equation. *Int. J. Therm. Sci.*, 103, 67–76. https://doi.org/10.1016/j.ijthermalsci.2015.12.008
19. Ghomanjani, F., & Farahi, M. H. (2012). The Bézier control points method for solving delay differential equation. *Intell. Control Autom.*, 3(2), 188–196. https://doi.org/10.4236/ica.2012.32021
20. Hafez, M. A., Jameel, A. F., Akgul, A., Almuhur, E., Mistarihi, M. Z., Amen, S. G., Hussain, A. S., & Tashtoush, M. A. (2026). Statistical control points: Approximate methods for solving first order fuzzy initial value problems. *J. Stat. Appl. Probab.*, 15(3), 455–478. https://doi.org/10.18576/jsap/150307
21. Harir, A., Melliani, S., Chadli, L. S., & Minchev, E. (2020). Solutions of fuzzy fractional heat-like and wave-like equations by variational iteration method. *Int. J. Contemp. Math. Sci.*, 15(1), 11–35. https://doi.org/10.12988/ijcms.2020.91229
22. He, O., & Yi, W. (1989). On fuzzy differential equations. *Fuzzy Sets and Systems*, 32(3), 321–325. https://doi.org/10.1016/0165-0114(89)90264-9
23. Jamal, N., Sarwar, M., Agarwal, P., Mlaiki, N., & Aloqaily, A. (2023). Solutions of fuzzy advection-diffusion and heat equations by natural adomian decomposition method. *Sci. Rep.*, 13(1), 18565. https://doi.org/10.1038/s41598-023-45207-y
24. Jameel, A. F. (2014). Semi-analytical solution of heat equation in fuzzy environment. *Int. J. Appl. Phys. Math.*, 4(6), 371–378. https://doi.org/10.17706/ijapm.2014.4.6.371-378
25. Jameel, A. F., Amen, S. G., Saaban, A., & Man, N. H. (2020). On solving fuzzy delay differential equation using bezier curves. *Int. J. Electr. Comput. Eng.*, 10(6), 6521–6530. https://doi.org/10.11591/ijece.v10i6.pp6521-6530
26. Jameel, A. F., Anakira, N., Alomari, A. K., Hashim, I., & Momani, S. (2016). A new approximation method for solving fuzzy heat equations. *J. Comput. Theor. Nanosci.*, 13(11), 7825–7832. https://doi.org/10.1166/jctn.2016.5784

27. Jameel, A. F., & Zureigat, H. H. (2015). Solution of fuzzy heat equations by homotopy perturbation method (HPM). *Asian J. Math. Comput. Res.*, 7(2), 127–139. https://ikprress.org/index.php/AJOMCOR/article/view/384
28. Kaleva, O. (1987). Fuzzy differential equations. *Fuzzy Sets and Systems*, 24(3), 301–317. https://doi.org/10.1016/0165-0114(87)90029-7
29. Lieberman, G. M. (1996). *Second order parabolic differential equations*. World Scientific. https://doi.org/10.1142/3302
30. Moore, R. E., Kearfott, R. B., & Cloud, M. J. (2009). *Introduction to interval analysis*. SIAM. https://doi.org/10.1137/1.9780898717716
31. Nittka, R. (2013). Quasilinear elliptic and parabolic Robin problems on Lipschitz domains. *NoDEA Nonlinear Differential Equations Appl.*, 20(3), 1125–1155. https://doi.org/10.1007/s00030-012-0201-2
32. Osman, M., Gong, Z., & Mustafa, A. M. (2020). Comparison of fuzzy Adomian decomposition method with fuzzy VIM for solving fuzzy heat-like and wave-like equations with variable coefficients. *Adv. Difference Equ.*, 2020(1), 327. https://doi.org/10.1186/s13662-020-02784-w
33. Seikkala, S. (1987). On the fuzzy initial value problem. *Fuzzy Sets and Systems*, 24(3), 319–330. https://doi.org/10.1016/0165-0114(87)90030-3
34. Sekhane, C., Laib, H., & Birem, F. (2026). Collocation scheme for 2D-VIEs with two constant delays. *Gulf J. Math.*, 23(1), 1–15. https://doi.org/10.56947/t8ty3q80
35. Trefethen, L. N. (2000). *Spectral methods in MATLAB*. SIAM. https://doi.org/10.1137/1.9780898719598
36. Wang, C., & Qiu, Z. P. (2014). Fuzzy finite difference method for heat conduction analysis with uncertain parameters. *Acta Mech. Sin.*, 30(3), 383–390. https://doi.org/10.1007/s10409-014-0036-7
37. Wu, J. (2012). Least squares methods for solving partial differential equations by using Bézier control points. *Appl. Math. Comput.*, 219(8), 3655–3663. https://doi.org/10.1016/j.amc.2012.09.063
38. Zadeh, L. A. (1965). Fuzzy sets. *Inform. and Control*, 8(3), 338–353. https://doi.org/10.1016/S0019-9958(65)90241-X
39. Zheng, J., Sederberg, T. W., & Johnson, R. W. (2004). Least squares methods for solving differential equations using Bézier control points. *Appl. Numer. Math.*, 48(2), 237–252. https://doi.org/10.1016/j.apnum.2002.01.001
40. Zimmermann, H. J. (1996). *Fuzzy set theory—and its applications* (3rd ed.). Springer. https://doi.org/10.1007/978-94-015-8702-0

[1] School of Mathematical Sciences, Universiti Sains Malaysia (USM), 11800 USM, Penang, Malaysia.
Email address: harranabuamro99@gmail.com

[2] School of Mathematical Sciences, Universiti Sains Malaysia (USM), 11800 USM, Penang, Malaysia; Nonlinear Dynamics Research Center (NDRC), Ajman University, Ajman, United Arab Emirates.
Email address: farahaini@usm.my

[3] Faculty of Education and Arts, Sohar University, Sultanate of Oman.
Email address: AJassar@su.edu.om

[4] School of Mathematical Sciences, Universiti Sains Malaysia, Penang, 11800 USM, Malaysia.
Email address: adilaazahar@usm.my

[5] School of Mathematical Sciences, Universiti Sains Malaysia (USM), 11800 USM, Penang, Malaysia.
Email address: Moath.alzoubi@yahoo.com